Multi-Composite Wavelet Estimation

Glenn R. Easley[a], Demetrio Labate[b], Vishal .M. Patel[c]

[a] System Planning Corporation, Arlington, Virginia
[b] University of Houston, Houston, Texas
[c] University of Maryland, College Park, Maryland

ABSTRACT

In this work, we present a new approach to image denoising derived from the general framework of wavelets with composite dilations. This framework extends the traditional wavelet approach by allowing for waveforms to be defined not only at various scales and locations but also according to various orthogonal transformations such as shearing transformations. The shearlet representation is, perhaps, the most widely known example of wavelets with composite dilations. However, many other representations are obtained within this framework, where directionality properties are controlled by different types of orthogonal matrices, such as the newly defined hyperbolets. In this paper, we show how to take advantage of different wavelets with composite dilations to sparsely represent important features such as edges and texture independently, and apply these techniques to derive improved algorithms for image denoising.

Keywords: W avelets, directional filter banks, wavelets with composite dilations, contourlets, shearlets, curvelets.

1. INTRODUCTION

It is widely acknowledged that wavelets provide a very effective representation for a large class of signals and images. However, a need for better directionally oriented filtering in order to improve multidimensional data processing was early recognized.[1–3] By conceiving a model of cartoon-like images as representative of piecewise-smooth functions that are smooth away from a C^2 edge, multi-scale and multi-directional representations were developed which exhibit near optimal approximations[4] and outperform traditional wavelet methods. Some of the most notable of these representations are the *curvelets*,[4,5] the *contourlets*[6] and the *shearlets*.[7,8]

The theory of *wavelets with composite dilations* is a generalization of the classical theory from which traditional wavelets are derived, and it provides a very flexible setting for the construction of many truly multidimensional variants of wavelets.[7,9,10] The most prominent construction derived from this approach is the shearlet representation. In this work, we present several new constructions of wavelets with composite dilations as well as a general algorithm for their implementations. Not only many of these new devised transforms demonstrate to be highly competitive in imaging applications; in addition this novel algorithmic technique, when adjusted to implement the shearlet transform, ends up improving the performance over the original shearlet transform implementation.[11]

For applications such as image denoising it is usually highly beneficial to use redundant (nonsubsampled) representations. Thus, keeping this observation in mind, we introduce a novel filter bank construction technique with no subsampling. This approach allows the projection of the data directly onto the desired directionally-oriented frequency subbands. An important novel feature of this construction is the ability to generate the decomposition atoms (frame elements) by directly applying the wavelet with composite dilations generating structure. This generating structure is given by particular combinations of matrix multiplications. Not only do these new implementation techniques follow very directly from the theoretical setting, they also allow for very sophisticated composite wavelet transforms to be carried out in the finite discrete setting.

As special cases of our approach, we introduce a new class of *hyperbolic* composite wavelet transforms which have potentially high impact in deconvolution and other image enhancement applications, as indicated by the novel decompositions suggested in Ref. 12 and by the techniques for dealing with motion blur recently proposed in Ref 13.

G.R.E. : E-mail: geasley@sysplan.com, D.L.: dlabate@math.uh.edu, V.M.P.: E-mail: pvishalm@umiacs.umd.edu

2. WAVELETS WITH COMPOSITE DILATIONS

The following notation and terminology will be used through this work. For $f \in L^2(\mathbb{R}^2)$, the *translation operator* T_τ is given by

$$T_\tau f(x) = f(x - \tau), \quad \tau \in \mathbb{R}^2.$$

Given an invertible matrix a on $\mathbb{R}^2$, the *dilation operator* D_a is defined as

$$D_a f(x) = |\det a|^{-1/2} f(a^{-1}x).$$

Given a set of generating function $\Psi = \{\psi_1, \ldots, \psi_L\} \subset L^2(\mathbb{R}^2)$ and a collection of 2×2 invertible matrices $A = \{a^i : i \in \mathbb{Z}\}$, the *wavelet systems* are the collections of functions of the form

$$\mathcal{A}_A(\Psi) = \{D_a T_k \psi_m : a \in A, \, m = 1, \ldots, L\},$$

when they form a Parseval frame for $L^2(\mathbb{R}^2)$. That is,

$$\|f\|^2 = \sum_{a \in A} \sum_{k \in \mathbb{Z}^2} |\langle f, D_a T_k \Psi \rangle|^2,$$

for all $f \in L^2(\mathbb{R}^2)$. Traditional wavelet systems are obtained in the special case where $a = 2\,I$, for I being the 2×2 identity matrix.

The *wavelets with composite dilations*[7] differ from standard wavelet systems by including a second set of dilations. In particular, they have the form

$$\mathcal{A}_{AB}(\Psi) = \{D_a D_b T_k \Psi : k \in \mathbb{Z}^n, \, a \in A, \, b \in B\},$$

where $A, B \subset GL_2(\mathbb{R})$ (where $GL_2(\mathbb{R})$ denotes the group of invertible matrices over $\mathbb{R}^2$) and the matrices $b \in B$ satisfy $|\det b| = 1$.

Analogous to standard wavelet systems, $\Psi \subset L^2(\mathbb{R}^2)$ is chosen so that

$$\|f\|^2 = \sum_{a \in A} \sum_{b \in B} \sum_{k \in \mathbb{Z}^2} |\langle f, D_a D_b T_k \Psi \rangle|^2,$$

for any $f \in L^2(\mathbb{R}^2)$. The matrices $a \in A$ are typically chosen to be expanding (but not necessarily isotropic, as in the traditional wavelet case) and the matrices $b \in B$ are associated with rotations and other orthogonal transformations.

The theory of wavelets with composite dilations extends many of the standard results of wavelet theory[7, 9, 10] and it allows to construct wavelet-like representation systems with a much richer choice of geometrical features.

To show that there plenty of examples of such systems, we recall this simple result from Ref. 9. Let ψ be chosen such that $\hat{\psi} = \chi_S$, where $S \subset \mathbb{R}^2$ and χ_S denotes the characteristic function of S. Then there are simple conditions for the constructions of composite wavelets:

THEOREM 2.1. *Let $\psi = (\chi_S)^\vee$ and suppose that $S \subset E \subset \mathbb{R}^2$. Suppose that $A, B \subset GL_2(\mathbb{R})$ satisfy*

1. $\widehat{\mathbb{R}}^2 = \bigcup_{k \in \mathbb{Z}^2} (E + k)$;

2. $\widehat{\mathbb{R}}^2 = \bigcup_{a \in A, b \in B} S\,(ab)^{-1}$,

where the union is essentially disjoint. Then the system

$$\mathcal{A}_{AB} = \{D_a D_b T_k \psi : k \in \mathbb{Z}^n, \, a \in A, \, b \in B\},$$

is a Parseval frame for $L^2(\mathbb{R}^2)$. If, in addition, $\|\psi\| = 1$, then $\mathcal{A}_{AB}$ is an orthonormal basis for $L^2(\mathbb{R}^2)$. Clearly, the systems obtained from the theorem above are not local in space domain. To achieve well-localized wavelets with composite dilations ad hoc constructions are needed, such as the shearlets in Ref. 14 or the constructions described in Ref. 15. Some additional novel well-localized constructions are introduced in this paper.

3. EXAMPLE CONSTRUCTIONS

Before presenting our new well-localized constructions, let us illustrate how to use Theorem 2.1, to derive some useful examples of wavelets with composite dilations for $L^2(\mathbb{R}^2)$.

3.1. Construction 1. Shearlet tiling

An important example of a wavelets with composite dilations is obtained by using dilation matrix $a = \left(\begin{smallmatrix} 2 & 0 \\ 0 & 2 \end{smallmatrix}\right)$ and B as the set $\{b^\ell : -3 \leq \ell \leq 2\}$ where b is the shear matrix $\left(\begin{smallmatrix} 1 & 1 \\ 0 & 1 \end{smallmatrix}\right)$. By letting R be the union of the trapezoid with vertices $(\frac{1}{2}, 0), (1, 0), (\frac{1}{2}, \frac{1}{6}), (1, \frac{1}{3})$ and the symmetric one with vertices $(-\frac{1}{2}, 0), (-1, 0), (-\frac{1}{2}, -\frac{1}{6}), (-1, -\frac{1}{3})$, and setting $\hat{\psi}^m(\xi) = \chi_{R_m}(\xi)$, where $R_m = R\, b^m$, it follows that the system

$$\mathcal{A}_0 = \{D_a^i\, D_b\, T_k\, \psi^m : i \geq 0,\, b \in B,\, k \in \mathbb{Z}^2, m = 1, 2, 3\}$$

is a Parseval frame for $L^2(\mathcal{D}_0)^\vee = \{f \in L^2(\mathbb{R}^2) : \operatorname{supp} \hat{f} \subset \mathcal{D}_0\}$, where $\mathcal{D}_0 = \{(\omega_1, \omega_2) : |\omega_2/\omega_1| \leq 1, |\omega_1| > 1\}$. To obtain a Parseval frame for the entire space $L^2(\mathbb{R}^2)$, first one can add a similar system

$$\mathcal{A}_1 = \{D_a^i\, D_b\, T_k\, \tilde{\psi}^m : i \geq 0,\, b \in \tilde{B},\, k \in \mathbb{Z}^2, m = 1, 2, 3\},$$

where $\tilde{B} = \{(b^T)^\ell : -3 \leq \ell \leq 2\}$. This is a Parseval frame for $L^2(\mathcal{D}_1)^\vee$ where $\mathcal{D}_1 = \{(\omega_1, \omega_2) : |\omega_2/\omega_1| \geq 1, |\omega_2| > 1\}$. Finally, it easy to construct an orthonormal basis $\Phi = \{T_k\, \phi : k \in \mathbb{Z}^2\}$ for $L^2([-\frac{1}{2}, \frac{1}{2}]^2)^\vee$. Hence, $\mathcal{A}_0 \cup \mathcal{A}_1 \cup \Phi$ is a Parseval frame of $L^2(\mathbb{R}^2)$.

This system was originally introduced in Ref. 7 and its frequency tiling is illustrated in Figure 1.
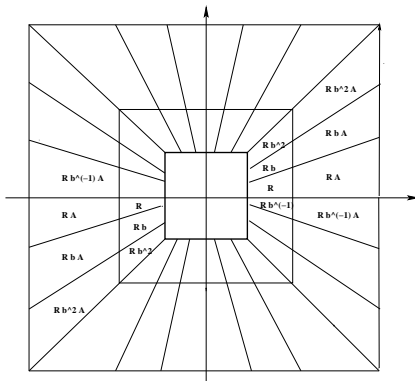

Figure 1. *Tiling of the spatial-frequency domain associated with a system of wavelets with composite dilations where $a = 2I$ where I is the 2×2 identity matrix and B are the shearing matrices.*

3.2. Construction 2. Hyperbolic tiling

Another example of wavelets with composite dilations is obtained by using matrices B of the form

$$B = \{b_\ell = \begin{pmatrix} \lambda^{-\ell} & 0 \\ 0 & \lambda^\ell \end{pmatrix} : \ell \in \mathbb{Z}\},$$

where $\lambda > 1$ is a fixed parameter. This construction can be seen as a transformation of the shearlet tiling under a nonlinear change of coordinates. In the following, we will set $\lambda = \sqrt{2}$, but the discussion below can be easily extended to other choices for λ.

For each $k > 0$, the set $H_k = \{(\xi_1, \xi_2) \in \widehat{\mathbb{R}}^2 : \xi_1 \xi_2 = k\}$ consists of two branches of hyperbolas. Notice that, for any $\xi = (\xi_1, \xi_2) \in H_k$, every other point ξ' on the same branch of hyperbola has the unique representation

3

$\xi' = (\xi_1 \gamma^{-t}, \xi_2 \gamma^t)$, where $\gamma > 1$ is fixed, for some $t \in \mathbb{R}$. This means any $\xi = (\xi_1, \xi_2)$ in the first quadrant can be parametrized by

$$\xi(r, t) = (\sqrt{r}\,(\sqrt{2})^{-t}, \sqrt{r}\,(\sqrt{2})^t),$$

where $r \geq 0$, $t \in \mathbb{R}$. This implies that

$$r = \xi_1 \xi_2, \quad 2^t = \frac{\xi_2}{\xi_1}.$$

For any $k_1 < k_2$, a set $\{\xi(r, t) : k_1 \leq r < k_2\}$ is an *hyperbolic strip* and, for $m_1 < m_2$, a set $\{\xi(r, t) : k_1 \leq r < k_2, m_1 \leq 2^t \leq m_2\}$ is an *hyperbolic trapezoid*.

For any $k \neq 0$, the action of B on the right preserves the hyperbolas H_k since

$$\xi\, b_\ell = (\xi_1, \xi_2) \begin{pmatrix} (\sqrt{2})^{-\ell} & 0 \\ 0 & (\sqrt{2})^\ell \end{pmatrix} = (\xi_1 (\sqrt{2})^{-\ell}, \xi_2 (\sqrt{2})^\ell) = (\eta_1, \eta_2),$$

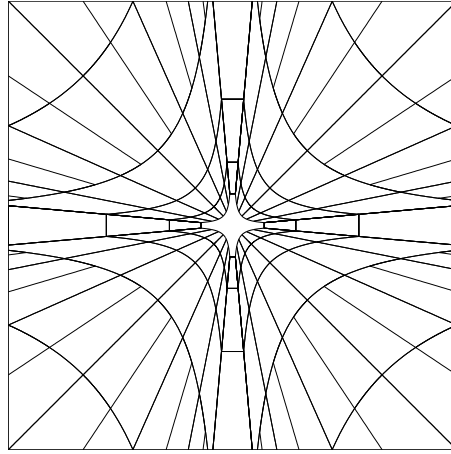and $\eta_1 \eta_2 = \xi_1 \xi_2$. Hence, the right action of B maps an hyperbolic strip into itself.

Figure 2. *Tiling of the frequency domain associated with an hyperbolic system of wavelets with composite dilations.*

Next let $A = \{a^i : i \in \mathbb{Z}\}$, where $a = \begin{pmatrix} \sqrt{2} & 0 \\ 0 & \sqrt{2} \end{pmatrix}$. Since a maps the hyperbola $\xi_1 \xi_2 = k$ to the hyperbola $\xi_1 \xi_2 = 2k$, it follows that a^i maps the hyperbolic strip $\{\xi(r, t) : 1 \leq r < 2\}$ to the hyperbolic strip $\{\xi(r, t) : 2^i \leq r < 2^{i+1}\}$. By defining a set of generators Ψ consisting of characteristic of appropriate sets in the frequency domain, it can be established that the hyperbolic system of wavelets with composite dilations $\{D_a^i D_{b_\ell} T_k \Psi : k \in \mathbb{Z}^2, \ell \in \mathbb{Z}\}$ is a Parseval frame of $L^2(\mathbb{R}^2)$. We refer to Ref. 16 for additional detail about this construction.

Notice that, as the value ℓ increases in magnitude, the hyperbolic trapezoids become increasingly narrow and asymptotically approach either the horizontal or the vertical axis. Hence, to realize the system in the finite discrete setting, the indices i and ℓ can be limited to a finite range and the asymptotic regions not covered because of this discretization can then be dealt with by partitioning up the complement with a Laplacian Pyramid filtering. An example of the tiling of the frequency plane associated with this construction is illustrated in Figure 2.

3.2.1. Well-localized Construction

To construct hyperbolic systems of wavelets with composite dilations (using the same matrices A and B given above) which are well-localized, it is important to recall the following useful result from Ref. 9.

THEOREM 3.1. *Let* $\psi \in L^2(\mathbb{R}^2)$ *be such that* $\operatorname{supp} \hat{\psi} \subset Q = [-\frac{1}{2}, \frac{1}{2}]^2$, *and*

$$\sum_{i,\ell \in \mathbb{Z}} |\hat{\psi}(\xi \, a^i \, b^\ell)|^2 = 1 \quad a.e. \ \xi \in \widehat{\mathbb{R}}^2,$$

where $a, b \in GL_n(\mathbb{R})$. *Then the system of wavelets with composite dilations* (1), *where* $A = \{a^i : i \in \mathbb{Z}\}$ *and* $B = \{b^j : j \in \mathbb{Z}\}$, *is a Parseval frame of* $L^2(\mathbb{R}^2)$.

Assuming $\xi_1 \xi_2 \geq 0$, $\xi_1 \neq 0$, let $\hat{\psi}$ be defined by

$$\hat{\psi}(\xi_1, \xi_2) = V(\xi_1 \xi_2) \, W(\frac{\xi_2}{\xi_1}),$$

where $V, W \in C_c^\infty(\mathbb{R})$ satisfy:

$$\sum_{i \in \mathbb{Z}} |V(2^i r)|^2 = 1 \quad \text{for a.e. } r \geq 0$$

$$\sum_{\ell \in \mathbb{Z}} |W(2^\ell 2^t)|^2 = 1 \quad \text{for a.e. } t \in \mathbb{R},$$

with $\operatorname{supp} V \subset [\frac{1}{16}, \frac{1}{2}]$ and $\operatorname{supp} W \subset [1, 2]$.

The functions V and W can be chosen to be basically Meyer wavelets that are restricted to the positive axis in the Fourier domain.

The well-localized system described above can be made to have a frequency footprint which is essentially given by Figure 2. The main difference is that the frequency supports of the different waveforms $\psi(a^i b^\ell x)$ now overlap. Thus, Figure 2 should now be interpreted as a picture of the essential frequency support.

When enforcing a parabolic scaling, the construction should be modified as follows: Let $\mathcal{D}_0 = \{(\xi_1, \xi_2) \in \widehat{\mathbb{R}}^2 : |\xi_1| \geq \frac{1}{16}, \left|\frac{\xi_2}{\xi_1}\right| \leq 1\}$ and $\mathcal{D}_1 = \{(\xi_1, \xi_2) \in \widehat{\mathbb{R}}^2 : |\xi_2| \geq \frac{1}{16}, \left|\frac{\xi_1}{\xi_2}\right| \leq 1\}$. Define $\hat{\Psi}^0$ to be $\hat{\Psi}$ restricted to $\mathcal{D}_0$ so that the collection $\{\hat{\Psi}^{(0)}(\xi a^i b_\ell)\}$ generates a tiling for $\mathcal{D}_0$ when $a = \begin{pmatrix} 2 & 0 \\ 0 & \sqrt{2} \end{pmatrix}$. Similarly, define $\hat{\Psi}^1$ to be $\hat{\Psi}$ restricted to $\mathcal{D}_1$ so that the collection $\{\hat{\Psi}^{(1)}(\xi a^i b_\ell)\}$ generates a tiling for $\mathcal{D}_1$ when $a = \begin{pmatrix} \sqrt{2} & 0 \\ 0 & 2 \end{pmatrix}$. The union of these collections, together with a system taking care of the low frequency region, then forms a complete tiling of $\widehat{\mathbb{R}}^2$.

4. COMPOSITE WAVELET IMPLEMENTATION

We now illustrate a general procedure for the numerical implementations of a large family of wavelets with composite dilations. As will be discussed below, the main goal is to devise a method to provide the appropriate partition of the frequency plane.

4.1. Analysis Filter Design

In this section, we introduce an approach for the construction of filters that match the spatial frequency tiling associated with the desired system of wavelets with composite dilations. In particular, given a system of wavelets with composite dilations $\mathcal{A}_{AB}(\Psi)$ with matrices A and B, this approach will directly apply the matrices A and B to generate the specific spatial frequency tiling associated with the system $\mathcal{A}_{AB}(\Psi)$. In this way, the discrete implementation provides a perfect match with its theoretical counterpart and it allows one to deal even with wavelets with composite dilations associated with very complicated geometrical decompositions in the spatial frequency plane.

To illustrate this approach, first let us consider a wavelet $\hat{\psi}(\xi) = \chi_S(\xi)$, where S corresponds to a bounded region satisfying the conditions of Theorem 2.1. For example, S can be chosen to be a trapezoidal hyperbola as given in Construction 2. A sequence of points $\{(\xi_1^n, \xi_2^n)\}_{n=1}^N \in S$ is then generated that densely fills the set S. We define $(\bar{\xi}_1^n, \bar{\xi}_2^n) = \lceil (\xi_1^n, \xi_2^n) \rceil$ where $\lceil \cdot \rceil$ denotes the ceiling function. The non-zero entries of our starting
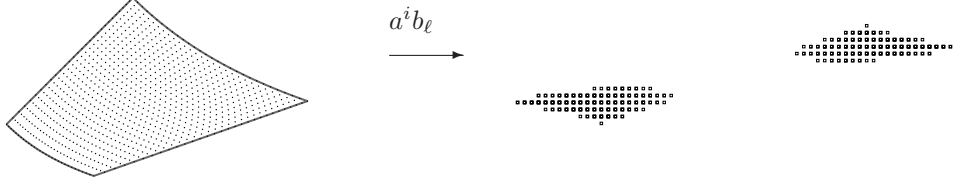
Figure 3. Illustrations of filter constructions where the number of samples used are small for the purpose of presentation. The images on the left are the sequences of points $\{(\xi_1^n, \xi_2^n)\}_{n=1}^N$ contained in the region S. The images on the right are the sequences of points $\{(\overline{\eta}_1^n, \overline{\eta}_2^n)\}_{n=1}^N$ where $(\overline{\eta}_1^n, \overline{\eta}_2^n) = \lceil (\xi_1^n, \xi_2^n) a^i b_\ell \rceil$.
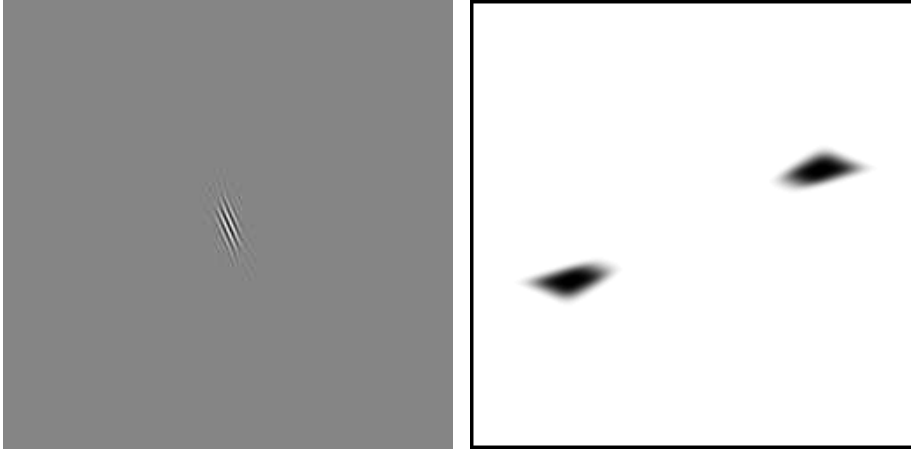

Figure 4. *An example of a hyperbolic filter. From left to right: Time Domain, Frequency Domain*

filter $\widehat{G}_{0,0}$ is to be created by the assignment $\widehat{G}_{0,0}(\overline{\xi}_1^n, \overline{\xi}_2^n) = 1$. Similarly, the filters $\{\widehat{G}_{i,\ell}\}$ are found assigning the non-zeros entries as $\widehat{G}_{i,\ell}(\overline{\eta}_1^n, \overline{\eta}_2^n) = 1$ for $(\overline{\eta}_1^n, \overline{\eta}_2^n) = \lceil (\xi_1^n, \xi_2^n) a^i b_\ell \rceil$. Observed that N needs to be chosen large enough so that the points $(\overline{\eta}_1^n, \overline{\eta}_2^n)$ are dense enough to fill out the regions $S_{i,\ell} = S a^i b_\ell$ completely in terms of its pixelated image for all desired values of i and ℓ. An illustration of this construction is provided in Figure 3.

The well-localized version of wavelets of composite dilations can be done by keeping track of the multiple assigned grid points. In this way, the windowing can be appropriately compensated by assigning the average windowed value at these point locations. Examples of this construction are shown in Figure 4.

4.2. Synthesis Filter Design

We will construct the synthesis filters by using a method devised for solving a related problem known as the Multichannel Deconvolution Problem (MDP) which can roughly be stated as follows. *Given a collection $\{G_i\}_{i=1}^m$ of distributions on $\mathbb{R}^d$ ($d \geq 2$), find a collection $\{\tilde{G}_i\}_{i=1}^m$ of distributions such that*

$$\sum_{i=0}^{m-1} \tilde{G}_i * G_i = \delta,$$

6

where δ is a Dirac delta distribution.

When the distributions are assumed to be compactly supported, this equation is referred to as the *analytic Bezout equation* when stated from the Fourier-Laplace domain. There is connection with the polynomial Bezout equation which is usually solved for computing the filters associated with traditional filter banks.[19]

Several methods for solving this problem in a discrete setting provide a way of constructing appropriate synthesis filters.[17–24] We will use the method given in Ref. 19 when small finite supported filters are desired.

Another solution to achieve perfect recontruction is to slightly modify the analysis filters to be

$$\widehat{G_i}(\xi_1, \xi_2) = \frac{\widehat{G_i}(\xi_1, \xi_2)}{\sqrt{\sum_{k=0}^{m-1} |\widehat{G_k}(\xi_1, \xi_2)|^2}}, \tag{1}$$

and to use

$$\widehat{\tilde{G}_i}(\xi_1, \xi_2) = \frac{\overline{\widehat{G_i}}(\xi_1, \xi_2)}{\sqrt{\sum_{k=0}^{m-1} |\widehat{G_k}(\xi_1, \xi_2)|^2}}, \tag{2}$$

as the synthesis filters for $i = 0, \ldots, m-1$.

Since the implementations of these composite wavelets will consists of m convolutions, the transforms will run in $O(N^2 \log N)$ operations for an $N \times N$ image.

Notice that the implementations of these composite wavelets form a tight frame when using (1) and (2), that they obtain perfect reconstructions, and that they are faithful in the sense that they ensure the spatial-frequency tiling prescribed by their continuous formulation. When dealing with the improved shearlet implementation, this new design is particularly appealing, since it removes any concern regarding the conversion between the Cartesian and the Pseudo-Polar domain (such as its norm preservation), and all its analogous properties in the finite discrete domain match their continuous counterparts.

5. IMAGE DENOISING

To illustrate the advantages of employing wavelets with composite dilations in imaging applications, we will present some applications to image denosing.

Given noisy observations

$$y = x + n,$$

where n is zero-mean white Gaussian noise with variance σ^2, the objective is to estimate x. One approach consists in estimating the image x via α by solving the following optimization problem:

$$\hat{\alpha} = \min_{\alpha} \|\alpha\|_1 \ \text{ subject to } \ \|W\alpha - y\|_2^2 \leq \epsilon, \tag{3}$$

where W is the composite wavelets dictionary used to represent an image. The threshold ϵ is related to the noise power. Once the sparse coefficients that represent the desired clean image are obtained, the denoised output is obtained by $\hat{x} = W\hat{\alpha}$.

Often times an image of interest may contain textured components along with piecewise smooth components. Hence, we can assume that x is a superposition of two components. That is, $x = x_p + x_t$, where x_p and x_t are the piecewise smooth component and textured component of an image, respectively. It has been suggested that taking a multi-representation approach to denoise may result in improved estimates. Hence, we have decided to use a Gabor representation or a representation from a discrete cosine basis to sparsify the textured components and wavelets with composite dilations to represent the piecewise smooth parts of an image.

The main technique for obtaining the denoised estimate of x will be to solve components of the image by solving the following optimization problem:

$$\hat{x}_p, \hat{x}_t = \arg \min_{x_p, x_t} \lambda \|W^\dagger x_p\|_1 + \lambda \|D^\dagger x_t\|_1 + \gamma \, TV(x_p) + \frac{1}{2}\|y - x_p - x_t\|_2^2, \tag{4}$$

where $D^\dagger$ denotes the Moore-Penrose pseudo inverse of D and TV is the Total Variation. Once the denoised components are obtained, we get the final estimate as $\hat{x} = \hat{x}_p + \hat{x}_t$. One of the major advantages of using (4) is that it requires searching lower dimensional vectors rather than longer dimensional representation coefficient vectors.

6. EXPERIMENTS

We can now present several numerical experiments on image denoising, based on the approach described in the previous section, to demonstrate the effectiveness of the wavelets with composite dilations and their discrete implementation. For brevity in presentation, we focus on using the improved implementation of the shearlet transform using the method of Section 4. We refer the reader to Ref. 16 for an extensive evaluation of the denoising performances of alternative composite wavelets such as the hyperbolic-based ones.

We compare the denoising performance of our technique with a recent Stein-Block thresholding method[25] using curvelets. This method was shown to be nearly minimax over a large class of images in the presence of additive bounded noise. This method requires a threshold parameter which we set to the theoretical value 4.505 as derived in Ref. 25. Notice that this method was shown to outperform the standard wavelet and curvelet-based denoising techniques. Hence, we use it for baseline comparison in this paper. The peak signal-to-noise ratio (PSNR) is used to measure the performance of different transforms. Given an $N \times N$ image x and its estimate $\tilde{x}$, the PSNR in decibels (dB) is defined as

$$PSNR = 20 \log_{10} \frac{255N}{\|x - \tilde{x}\|_F},$$

where $\|.\|_F$ is the Frobenius norm.

Figure 5 and Figure 6 show the results of the denoising experiments where the new technique was generically labeled as NSWCD for NonSubsampled Wavelets with Composite Dilations. As can be seen from these figures, our approach to denoising which combines wavelets with composite dilations* and discrete cosine representations provides results that compare favourably to the ones obtained by using the Stein-Block thresholding method.

7. CONCLUSION

In this work, we have shown the framework of wavelets with composite dilations is capable of generating extremely useful multiscale and multidirectional decompositions. In particular, we have illustrated how to construct a new system of hypberbolic wavelets with composite dilations. To derive numerical implementations of these decompositions, a multichannel implementation was devised that allows the filters to be constructed directly from the generating structure. We have demonstrated the power of these transforms by demonstrating their ability to denoise images by using a component-based optimization formulation. The results demonstrate these new methods are extremely competitive with respect to other state-of-the-art methods.

ACKNOWLEDGMENTS

REFERENCES

1. R. H. Bamberger and M. J. T. Smith, A filter bank for directional decomposition of images: theory and design, *IEEE Trans. Signal Process.*, 40(2), pp. 882–893, 1992.
2. W. T. Freeman and E. H. Adelson, The design and use of steerable filters, *IEEE Trans. Patt. Anal. Mach. Intell.*, no. 9, pp. 891–906, September 1991.
3. E. P. Simoncelli and E. H. Adelson, Non-separable extensions of quadrature mirror filters to multiple dimensions, *Proceedings of the IEEE*, **78**, no. 4, pp. 652–664, April 1990.

---

*Shearlets were only used to demonstrated the technique yet other composite wavelets have proven to be effective as well.

(a)

(b)

(c)

(d)

Figure 5. Image denoising experiment with the *Boats* image. (a) Original image. (b) Noisy image (PSNR 22.94 dB). (c) Stein-Block-based estimate (PSNR = 27.17 dB). (d) NSWCD-based estimate (PSNR = 27.35 dB).
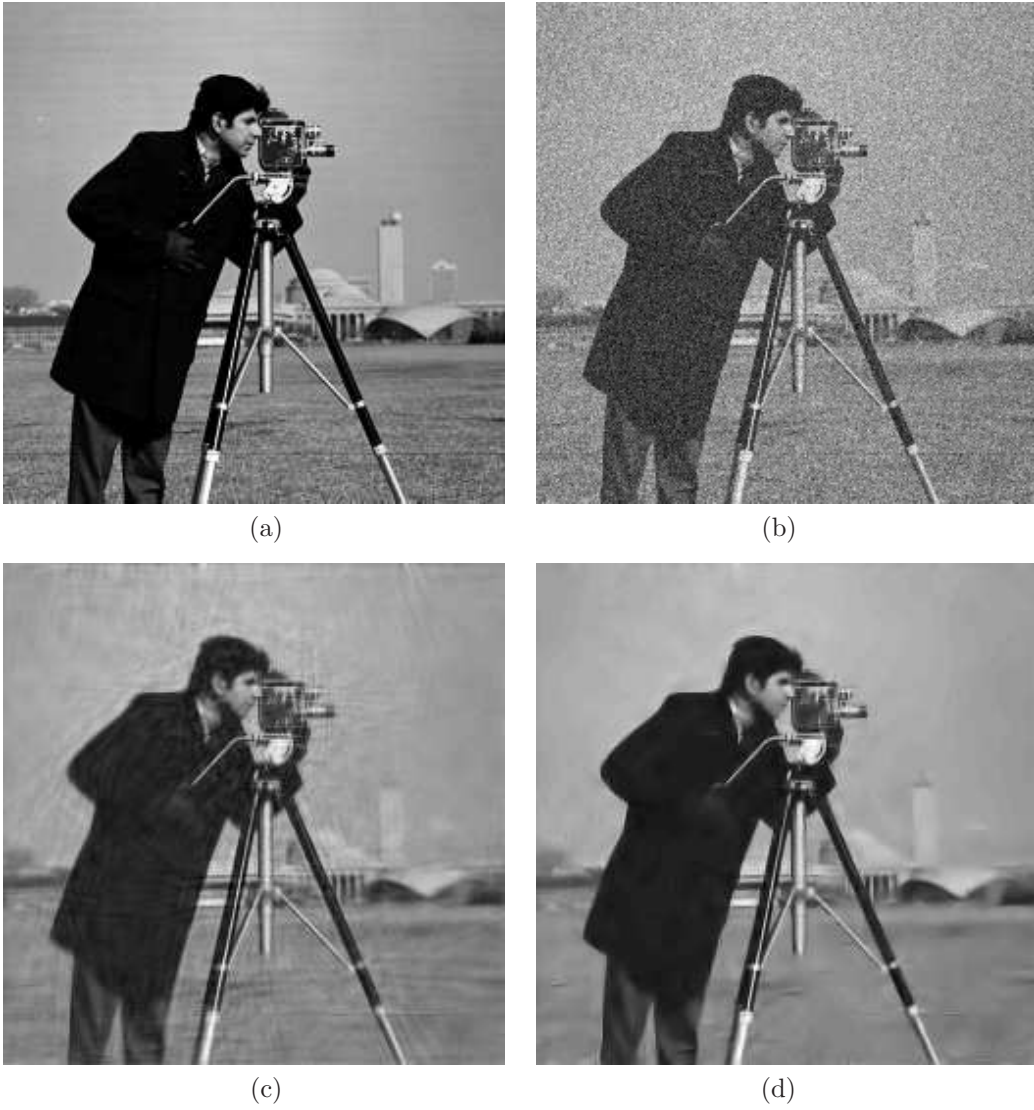
Figure 6. Image denoising experiment with the *Cameraman* image. (a) Original image. (b) Noisy image (PSNR 20.15 dB). (c) Stein-Block-based estimate (PSNR = 27.01 dB). (d) NSWCD-based estimate (PSNR = 27.96 dB).

4. E. J. Candès and D. L. Donoho, New tight frames of curvelets and optimal representations of objects with piecewise C^2 singularities, *Comm. Pure and Appl. Math.*, vol. 56, pp. 216–266, 2004.

5. J. L. Starck, E. J. Candès, and D. L. Donoho, The curvelet transform for image denoising, *IEEE Trans Image Process.*, vol. 11, no. 6, pp. 670–684, 2002.

6. M. N. Do and M. Vetterli, The contourlet transform: an efficient directional multiresolution image representation, *IEEE Trans. Image Process.*, vol. 14, no. 12, pp. 2091–2106, Dec. 2005.

7. K. Guo, D. Labate, W.-Q. Lim, D. Labate, G. Weiss, and E. Wilson, Wavelets with composite dilations, *Electron. Res. Announc. Amer. Math. Soc.*, vol. 10, pp. 78–87, 2004.

8. D. Labate, W. Lim, G. Kutyniok, and G. Weiss, Sparse multidimensional representation using shearlets, Wavelets XI (San Diego, CA, 2005), 254–262, SPIE Proc. **5914**, SPIE, Bellingham, WA, 2005.

9. ——, Wavelets with composite dilations and their MRA properties, *Appl. Comput. Harmon. Anal.*, vol. 20, pp. 220–236, 2006.

10. ——, The theory of wavelets with composite dilations in: *Harmonic Analysis and Applications, C. Heil (ed.), pp. 231–249.* Boston, MA: Birkhäuser, 2006.

11. G. Easley, D. Labate and W. Lim, Sparse Directional Image Representations using the Discrete Shearlet Transform, *Appl. Comput. Harmon. Anal.* **25** pp. 25-46, (2008)

12. J. Chung, G. R. Easley, and D. P. O'Leary, Windowed Spectral Regularization of Inverse Problems, *preprint*, 2010.

13. K. Egan, Y-T Tseng, N. Holzschuch, F. Durand, R. Ramamorthi, Frequency Analysis and Sheared Reconstruction for Rendering Motion Blur, *to appear in ACM SIGGRAPH*, 2011.

14. K. Guo and D. Labate, Optimally sparse multidimensional representation using shearlets, *SIAM J. Math. Anal.*, vol. 9, pp. 298–318, 2007.

15. G. Easley, D. Labate, Critically sampled wavelets with composite dilations, *to appear in IEEE Trans. on Imag. Processing*, 2011.

16. G. Easley, D. Labate, V. Patel, Directional multiscale processing of images using wavelets with composite dilations, preprint, 2011.

17. C. A. Berenstein, A. Yger, and B. A. Taylor, Sur quelques formules explicites de deconvolution, *Journal of Optics (Paris)* **14**, pp. 75–82, 1983.

18. C. A. Berenstein, and A. Yger, Le problème de la déconvolution, *J. Funct. Anal.*, pp. 113–160, 1983.

19. F. Colonna, and G. R. Easley, The multichannel deconvolution problem: a discrete analysis, *J. Fourier Anal. Appl.* **10**, pp. 351–376, 2004.

20. G. R. Easley, and D. F. Walnut, Local multichannel deconvolution, *J. Math. Imaging Vision* **18**, pp. 69-80, 2003.

21. G. Harikumar, and Y. Bresler, FIR perfect signal reconstruction from multiple convolutions: minimum deconvolver orders, *IEEE Transactions on Signal Proc.* **46**, pp. 215–218, 1998.

22. P. Schiske, Zur frage der bildrekonstruktion durch fokusreihen, *Proc. Eur. Reg. Conf. Electron. Microsc., 4th*, pp. 1–145, 1968.

23. P. Schiske, Image processing using additional statistical information about the object. In P. W. Hawkes, ed., *Image Processing and Computer Aided Design in Electron Optics*. Academic Press, New York, 1973.

24. J. Zhou, and M. N. Do, Multidimensional multichannel FIR deconvolution using Gröbner bases, *IEEE Trans. Image Proc.* **15**, pp. 2998–3007 , 2006.

25. C. Chesneau, J. Fadili and J-L. Starck, "Stein block thresholding for image denoising," *Applied and Computational Harmonic Analysis,* vol. 28, no. 1, pp. 67–88, 2010.